Stability optimisation of turbocharger rotor-floating ring bearing system: a combination of linear and nonlinear approaches

L. Tian[1], Y. Lu[2], J. M. Ramamoorthy[3], M. Wakelin[1], C. Lancaster[1]

1 Cummins Turbo Technologies, UK

2 Wuxi Cummins Turbo Technologies, China

3 Cummins Turbo Technologies, India

ABSTRACT

Rotordynamic stability is of the utmost importance in turbocharger (TC) floating ring bearing (FRB) system development. This is further emphasized by the continuous demand for higher operating speeds (up to 300 krpm) yet tougher lubrication conditions to meet the ever stringent emission regulations and to improve the engine fuel efficiency. Differing from other types of turbomachines, the dynamic behaviour of TC rotor-FRB system is characterised by high nonlinearity due to its inherent instability over most of its operating speed range. Understanding this highly nonlinear behaviour, which is deeply coupled with bearing structural configurations, entails more complex analysis techniques, e.g. nonlinear transient rotordynamic simulation, as the traditional linear analysis method showed limited capabilities. However, when running parametric optimisation studies considering all bearing structural parameters, the number of nonlinear transient simulations needed can be large. Accordingly, the required time for completing the study can easily become unacceptable. In an effort to deal with this challenge, this paper shows that, despite some limitations, the linear stability analysis method, with much less running time, can be effectively used as a qualitative pilot analysis tool to search for the optimised parameter space. More advanced nonlinear transient run-up simulations are then performed to virtually validate the found parameter space. The powerful combination of linear and nonlinear analysis methods can make the full parametric study feasible for stability optimisation. The optimised solution given by the presented approach is experimentally verified using correlation to measured shaft motion.

1. INTRODUCTION

Following the trend of down-sizing for better fuel economy and the consequential requirement for increased power density, turbochargers (TCs) have already become a key element of the automotive powertrain. In order to meet the ever stringent emission regulations and the persistent demand for better fuel efficiency, the design

and development of the rotor-floating ring bearing (FRB) system of TCs face several new challenges. For example, the running speed is increased, up to 300 krpm for passenger car applications, while in the meantime, the oil supply pressure becomes lower, as given by a smaller engine oil pump for improved system efficiency. The oil viscosity is also reduced with an extended oil drain interval to lower running costs. The deterioration of those running conditions imposes extra difficulty to achieve acceptable stability performance of the TC rotor-FRB system throughout the operating speed range. In addition, an acceptable rotor-FRB system design should meet the increasingly stringent requirement for synchronous and non-synchronous noise and for reduced frictional loss to deliver an improved overall TC efficiency. Those targets considering different aspects are sometimes directly contradictory to each other. For example, an increased bearing land length may be able to deliver improved stability over the high speed range, although it will also increase the bearing frictional losses (1). Additionally, the rotor vibration characteristics in the sub-synchronous region are likely to be influenced. A longer bearing land can intensify sub-synchronous vibration in the low speed range, which increases the noise level. These circumstances, in conjunction with the need of test cost reduction and shorter development time, strongly emphasize the necessity to develop a reliable and efficient simulation tool to fully understand the boundaries of existing TC rotor-bearing systems, and to provide an optimised design during new product development.

Historically, the development of TC rotor-FRB system was heavily dependent on test iterations. Given the high nonlinearity associated with oil film instability, the traditional linear analysis method, used for critical speed calculations, working well for majority of turbomachines, cannot provide quantitative correlation to the test results. Therefore, the time needed for product development is long and the cost is high. Excitingly, thanks to the availability of fast-growing computational power, significant progress in turbocharger rotordynamic simulation has been made in the last decade (2–8). Satisfactory agreement between simulation and test results has been achieved by nonlinear transient simulations, which solves a set of governing ordinary differential equations coupled by nonlinear bearing force calculations in a time stepping manner. The nonlinear bearing force model is at the heart of the simulation and can be deployed by different analytical and numerical techniques (6,9,10), which can significantly increase the simulation time if higher accuracy is preferred. Even though the simplest analytical nonlinear force model is used, depending upon the computing system, the simulation run at a single design point still needs hours to complete. This means that relying on the nonlinear transient simulation method to optimise the bearing design in a large parameter space including both geometrical and physical factors can become computationally intensive. By contrast, although the traditional linear analysis has been found to provide only limited information in regard to quantitative prediction, in Ref. (7) the first author showed that the unstable modes predicted by linear stability analysis can be correlated to the nonlinear jumps from the conical mode (Sub 1) to the cylindrical mode (Sub 2) and from the cylindrical mode (Sub 2) to another conical mode (Sub 3). It was also shown that the linear prediction for more complex nonlinear behaviour at higher speeds is not useful, especially for predicting the onset speed of the so-called critical limit cycle (CLC) oscillation, which is the synchronised instability of both inner and outer oil films (9,11–13). However, it was identified that the value of logarithmic decrement can show the qualitative trend of stability from a comparative point of view (7).

In an effort to develop an efficient TC rotordynamic simulation tool for parametric studies, this paper further exploits the linear stability analysis method. It will be shown in the following sections that, the method can be employed as a pilot indicator to assess the stability of the rotor-FRB system in the stage of parameter space

screening. As a result, an initial optimised parameter combination is obtained, which in turn enables the feasibility of nonlinear transient simulation to obtain quantitative information considering the required development time. Following this procedure, the initial results indicated by the linear stability analysis can also be checked and validated by the more time-consuming nonlinear transient analysis. The last step involves a correlation study between the simulated and tested results to verify the simulation oriented design.

This paper is structured as follows. The linear and nonlinear TC rotor-FRB model is briefly introduced in Sec. 2. The results of an example design given by the combined linear and nonlinear simulation approaches are presented in Sec. 3. Two correlation examples between nonlinear transient simulation and shaft motion measurement are detailed in Sec. 4, which is followed by a short conclusion given in Sec. 5.

2. MODEL DESCRIPTION

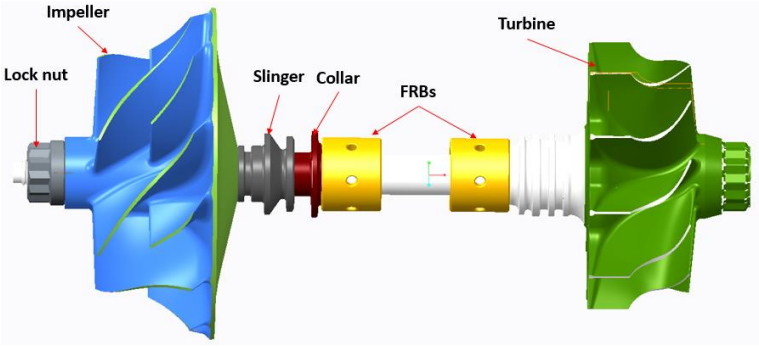

Figure 1: CAD model of the studied TC-FRB system

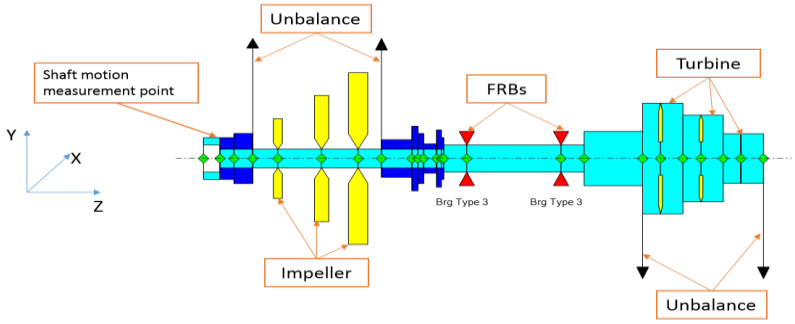

Figure 2: TC rotor-FRB FEM model

The CAD model of the TC rotating assembly under investigation including two FRBs is shown in **Fig. 1**. For rotordynamic analysis, the shaft is discretised as Timoshenko beam sections using the finite element method (FEM) developed in the toolbox according to Ref. (14), as depicted in **Fig. 2**. The turbine wheel is modelled as an integrated part of the shaft and is divided into three circular beam sections with additional inertia property values attached to match the analysed turbine wheel. The compressor wheel is also sliced into three portions which are modelled as rigid disks. Their mass and inertia properties are lumped to the locations on the shaft corresponding to the centre of gravity. It should be noted that, in the early stage of design, the complete CAD models of impeller and turbine wheel are not available, so

the mass and inertia properties of scaled models from existing design are used. This assumption is acceptable, as the difference from the final design has been proved minor. The smaller parts including lock nut, collar and slinger are only included in the last-step correlation study, as their effect on the overall dynamic response has been found insignificant in the presented example. The mathematical modelling of the bearing force from both FRBs can be realised linearly and nonlinearly, and it is detailed in the following subsections.

2.1 Linear TC rotor-FRB model

For linear stability analysis, it is assumed that the magnitude of the rotor vibration is small and the bearing forces for the two FRBs can be linearised as speed dependent stiffness and damping elements from its equilibrium position determined by bearing static load analysis under gravity. Thus, the two FRBs can be represented by two mass pedestals connected to rotor shaft and bearing housing by those linearised stiffness and damping elements, calculated using short bearing approximation (6,7). The linearised governing equations of motion for the investigated TC rotor-FRB system is given by

$$\mathbf{M}\ddot{\mathbf{q}}(\mathbf{t}) + (\mathbf{C} + \Omega\mathbf{G})\dot{\mathbf{q}}(\mathbf{t}) + \mathbf{K}\mathbf{q}(\mathbf{t}) = 0 \tag{1}$$

where $\mathbf{q}(\mathbf{t})$ is the response of the system from the static equilibrium position. **M** is the mass matrix of rotor assembly derived using FEM and includes the masses of the two FRBs. **C** is the damping matrix, in which the system external damping is considered negligible and only the bearing damping components are present to purely investigate the effect of bearing damping on the system stability. **K** denotes the system stiffness matrix including the contribution of bearing stiffness. Ω represents the rotor speed and $\mathbf{G}$ is the system gyroscopic matrix. Note that for linear stability analysis purpose, Eq. (1) is a free vibration problem and the unbalance forces are not shown on the right hand side of the equation. The solution of Eq. (1) has the exponential form

$$\mathbf{q}(\mathbf{t}) = \mathbf{u}e^{\lambda t} \tag{2}$$

After Eq. (2) is introduced into Eq. (1) and dividing both sides of the equation by $e^{\lambda t}$, the following eigenvalue problem is obtained

$$(\lambda^2\mathbf{M} + \lambda\mathbf{C} + \mathbf{K})\mathbf{u} = 0 \tag{3}$$

The eigenvalues λ in Eq. (3) are complex in general, and has the form

$$\lambda = \sigma + j\omega \tag{4}$$

where the real parts of eigenvalues σ are the damping exponents. A negative damping exponent means the corresponding solution given in Eq. (2) is exponentially decaying with time and the mode related to the damped natural frequency ω is said to be stable. In contrast, a positive σ means the corresponding solution is exponentially diverging with time. Thus, the mode of the associated natural frequency ω is considered unstable. The damping exponents σ is used as a stability indicator in the form of logarithmic decrements δ as follows (15).

$$\delta = -\sigma\left(\frac{2\pi}{\omega}\right) \tag{5}$$

where a negative δ indicates that the system is unstable. With respect to parameter variation and rotor speed change, a decreasing δ means the stability of the

associated mode at frequency ω is considered reduced, while an increasing δ means the system stability is improved.

2.2 Nonlinear rotor-FRB model

In nonlinear transient analysis, the governing equations of the motion given in Eq. (1) is modified as

$$\mathbf{M}\ddot{\mathbf{q}}(\mathbf{t}) + (\mathbf{C} + \Omega\mathbf{G})\dot{\mathbf{q}}(\mathbf{t}) + \mathbf{K}\mathbf{q}(\mathbf{t}) = \mathbf{F_b} + \mathbf{F_{ub}} + \mathbf{F_g} \quad (6)$$

where $\mathbf{q}(\mathbf{t})$ denotes the system response from the bearing centre line. It should be noted that the system damping matrix $\mathbf{C}$ and stiffness matrix $\mathbf{K}$ no longer include the bearing contribution in this case. Instead, the bearing force vector $\mathbf{F_b}$ is located on the right hand side of Eq. (6). What can also be seen are two additional items, the unbalance force vector $\mathbf{F_{ub}}$ and gravity vector $\mathbf{F_g}$. In this paper, a run-up procedure is deployed, so $\mathbf{F_{ub}}$ also includes the effect of rotor acceleration, of which the detailed expression can be found in Ref. (13). As to the bearing force calculation, two methods have been implemented. The analytical model derived from short bearing approximation as given in Ref. (6,7) is an efficient option, as the needed simulation time is much shorter than the numerical scheme based upon finite difference method (FDM) as described in Ref. (8). Including oil feeding conditions and full bearing geometry, The FDM model is considered more accurate and should be used when assessing the effect of more detailed lubrication conditions, for example, the relationship between oil inlet pressure and the dynamic response of the TC-FRB system. In this paper, only the analytical model is used for the nonlinear transient simulations shown in Sec. 3-4, and it will be proved sufficient for demonstrating the proposed method.

3. Linear parametric study and nonlinear validation

Table 1 TC rotor-FRB system physical parameters and oil inlet conditions

Parameters	Value
Rotor Mass	845 gram
Rotor Length	117 mm
Oil grade	SAE 20
Oil inlet pressure	2e5 Pa
Oil inlet temperature	105 °C
Rotor speed range	up to 220 krpm
FRB inner clearance (normalised by existing design)	0.78 ~ 1.65
FRB outer clearance (normalised by existing design)	0.84 ~ 1.40
FRB inner length (normalised by existing design)	1
FRB outer length (normalised by existing design)	1.125
FRB outer/inner radius ratio	1.8

The dynamic response of TC rotor-FRB system is known to be extremely sensitive to the bearing geometrical parameters (1,5,7,11). Prior to the linear stability analysis, the range of the bearing geometrical parameters are chosen based upon an existing bearing design, and one example of the evaluated parameter combinations is shown in **Table 1**. Note that the given values of the inner/outer clearance range and inner/outer length are normalised against the corresponding geometrical parameter of the existing bearing design. The FRB inner/outer length is fixed and only the effect of bearing clearance variations is investigated in this example. The same method can easily be extended to an enlarged parameter space.

3.1 Linear stability optimisation

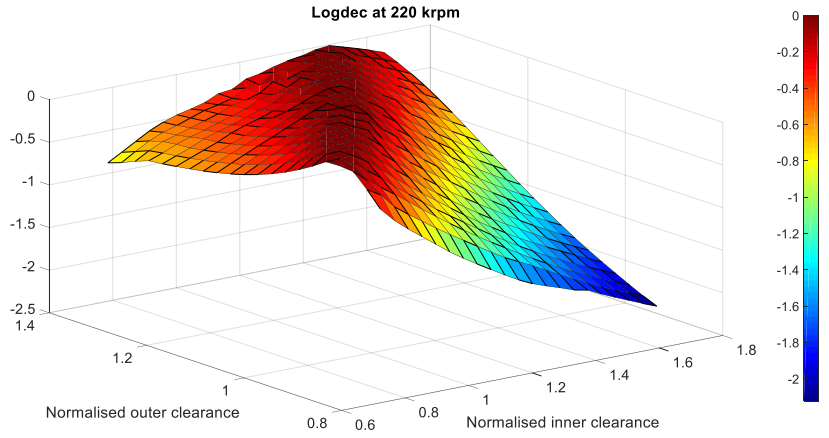

(a) 3D view

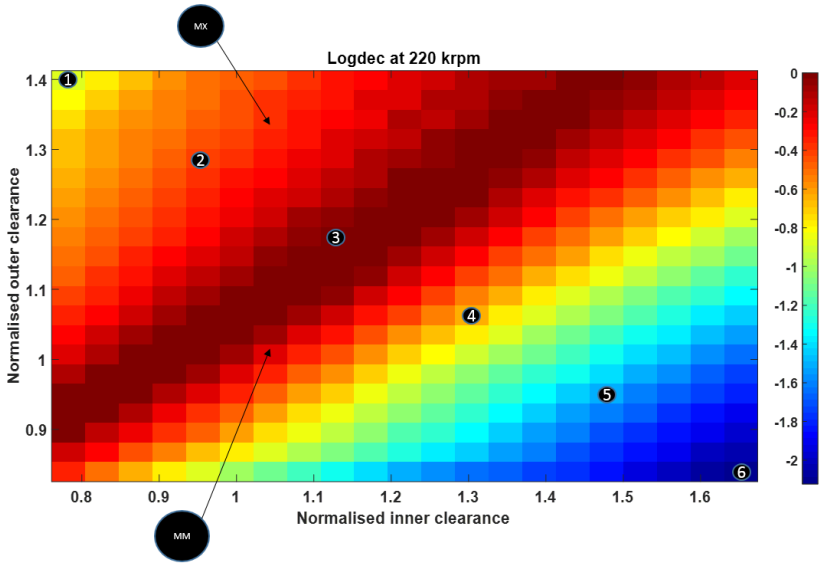

(b) 2D view

Figure 3 Minimum logarithmic decrement at 220 krpm over the defined inner/outer clearance range

The calculated minimum logarithmic decrement of the defined clearance range at 220 krpm is shown in **Fig. 3**. The following colour pattern corresponds to the ascending order of logarithmic decrement: dark blue, light blue, cyan, yellow, orange and red. Following the definition given by Eq. (5), it is seen that the most stable region is around the line connecting (0.8, 0.9) to (1.6, 1.4), despite the fact that the highest result is only marginally stable from the linear sense as the value is close to 0. It can also be observed that the two sides of the plateau region have rather different gradients. With increasing inner clearance but decreasing outer clearance, the logarithmic decrement value on the right slope decreases rapidly to the lowest point

as shown in **Fig. 3a**. Linearly speaking, considering the calculated absolute value of logarithmic decrement, this graph can be considered as a proof of the limitation of the linear analysis method for TC rotordynamic analysis. Accepting this truth, the authors will demonstrate that a qualitative direction for comparative analysis can still be obtained using the described method, which leads to invaluable insight into the degree of instability across the defined parameter space. It is worth noting that the centrifugal pumping loss due to the rotation of FRB should be carefully assessed across the speed range to avoid any risk of oil starvation to the inner film. Considering the scope of this paper, this effect is not included here, though the reader can refer to Ref. (16) for more information.

3.2 Validation through nonlinear run-up simulation

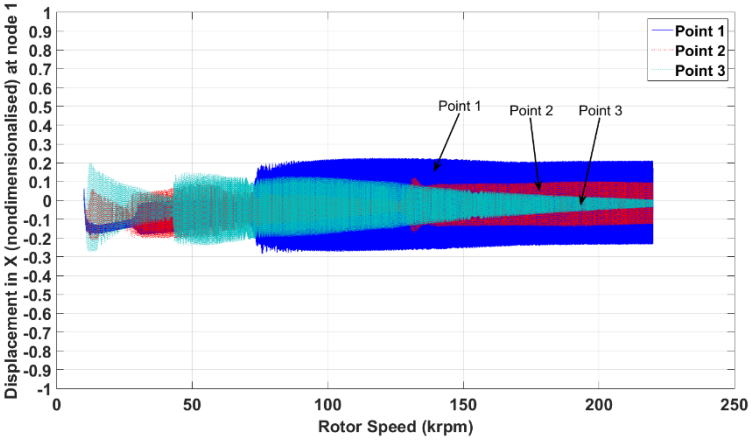

(a) The results from point 1 to point 3 in Fig. 3

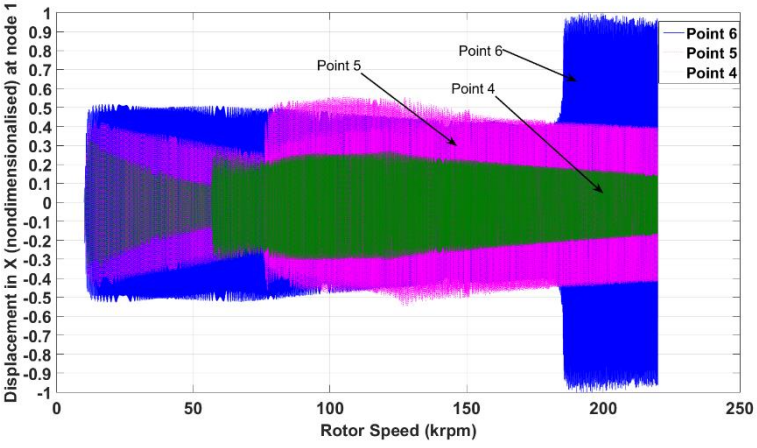

(b) The results from point 4 to point 6 in Fig. 3

Figure 4 Displacement plot of the selected points at compressor nose from nonlinear simulation; data is normalised against the maximum displacement amplitude at point 6.

In order to obtain qualitative information for the prediction given by linear stability analysis, nonlinear transient simulations are performed and the results are presented in this section. Six points predicted with marked variations of logarithmic decrement are selected from the defined parameter space as depicted in **Fig. 3b**. For the purpose of minimising the nonlinear interaction of unbalance (12), a quarter of the associated component unbalance limit are applied to four of the illustrated unbalance planes represented by black arrows in **Fig.2**.

The displacement plots in *X* according to **Fig. 2** at the compressor nose plane of the six selected points are given in **Fig. 4**. Note that all results are normalised against the predicted maximum amplitude of rotor displacement in *X* of point 6 at the same location. Those results are overlaid and plotted in two figures for clarity. The results from point 1 to point 3, and from point 4 to point 6 are shown in **Fig. 4a** and **4b**, respectively. It is clearly seen that point 3 gives the best results in terms of high speed dynamic response among all the simulated points. The predicted amplitude of the displacement at 220 krpm is less than 5 percent of the maximum amplitude given by point 6. The trend of the stability performance of the investigated rotor-FRB system given by the linear stability analysis is well correlated to the results from nonlinear transient simulation. It should be mentioned that point 3 does not give the lowest peak-to-peak displacement across the entire speed range, especially in the low speed range, although the level of displacement of point 3 is still comparable to point 1 and 2. What can also be seen is that the abrupt changes of the rotor displacement at different rotor speeds in the low speed region for each of the simulated cases. It can be explained by the so-called nonlinear jump phenomenon, which is normally associated with the sudden changes of the frequency and mode shape of the dominant sub-synchronous component in the frequency domain (5-7, 11, 13). In TC rotor-FRB system development, stability is of the greatest concern in the high speed region, as the dynamic loads are much higher and therefore poor stability performance can quickly cause rotor failure. This justifies choosing top speed as the target of stability optimisation.

4. Comparison between test results and selected design points

As discussed in Section 3, the final decision of a TC rotor-FRB design is subject to more considerations than just finding the optimal point which gives the lowest logarithmic decrement value in the parameter space. Compromise may be made when considering other aspects, for example, the tolerance of each bearing geometrical dimension. This means that the chosen bearing design is represented by a rectangular box covering the area determined by bearing inner/outer clearance tolerance rather than a single point in **Fig. 3b**. Thus, the stability across the entire box should be assessed properly using both linear and nonlinear simulation techniques, and the obtained results need to be further verified by shaft motion measurements on the gas stand. In order to complete the illustration of the method described in this paper, the correlation study between the test and simulation results of two selected corners of the defined bearing design (as shown in **Fig. 3b**) are given in **Fig. 5** and **6**. In those simulations, component unbalance limits are used for the associated balance planes as shown in **Fig. 2**. Considering the length of this paper, the definitions of the different sub-synchronous components are not given here, although detailed discussion can be found in Ref. (5,7,8,11,13).

4.1 Minimum inner clearance and minimum outer clearance (MM)

The predicted and measured results obtained at MM (min inner clearance/min outer clearance) tolerance box corner is given in **Fig. 5**. The simulation was started from 10 krpm, although the low speed region was removed in the plots for a direct comparison with test results. The measurement axis of the motion probe is not exactly aligned with the TC bearing centre. Thus the measured shaft motion normally

includes this initial eccentricity, which leads to a higher measured value than the simulated results. In order to minimise this effect, the predicted and measured results are normalised against the predicted and measured maximum displacement amplitude, respectively.

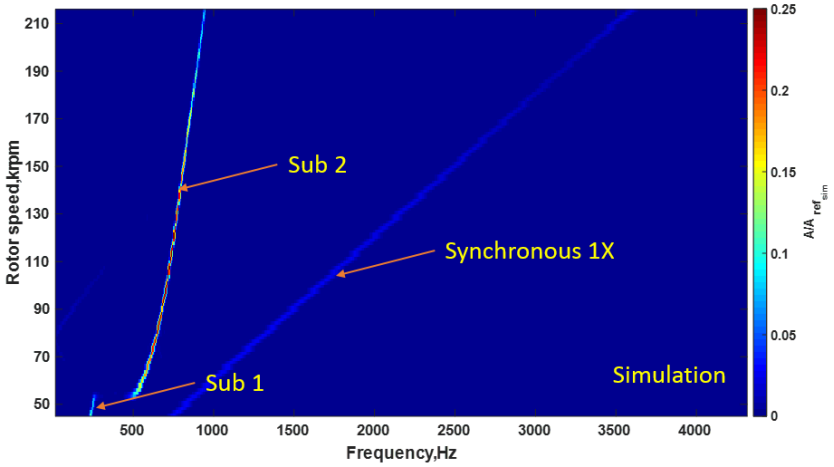

(a) Simulation results at MM

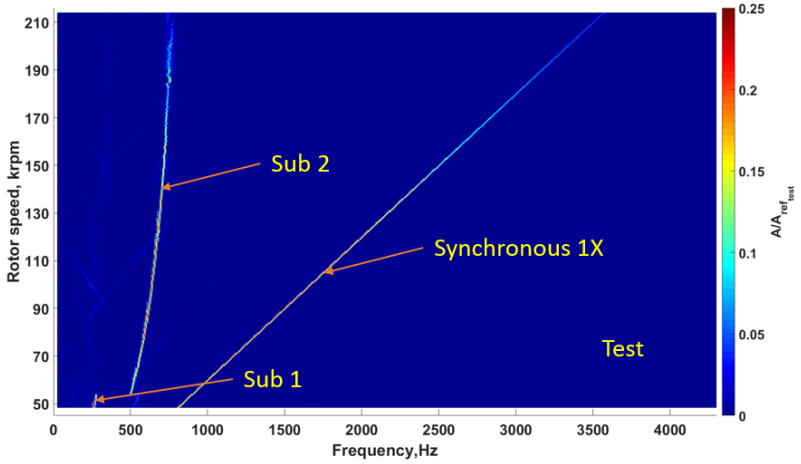

(b) Test results at MM

Figure 5 Waterfall diagrams of the simulated and measured rotor displacement at MM at the indicated shaft motion measurement point in Fig. 2 in *X*; the magnitude of the predicted and tested response are normalised by the predicted and measured maximum displacement amplitude, respectively.

It is seen that the simulation results are well correlated to the test results, especially in the sub-synchronous region. The main difference is observed when comparing the intensity of the synchronous component. The first reason could be given by the measurement error as described in the preceding paragraph. The second reason could be due to the fact that, following the high speed core balancing procedure, the exact unbalance distribution across the rotor of the tested unit is unknown. However,

the correlation between test and simulation is still considered good in this case, because the main rotordynamic characteristics revealed in the test are fully replicated by simulation, including the nonlinear jump from Sub 1 to Sub 2 at approximately 50 krpm, and the dominant but decaying effect of Sub 2 with increasing rotor speed.

4.2 Minimum inner clearance and maximum outer clearance (MX)

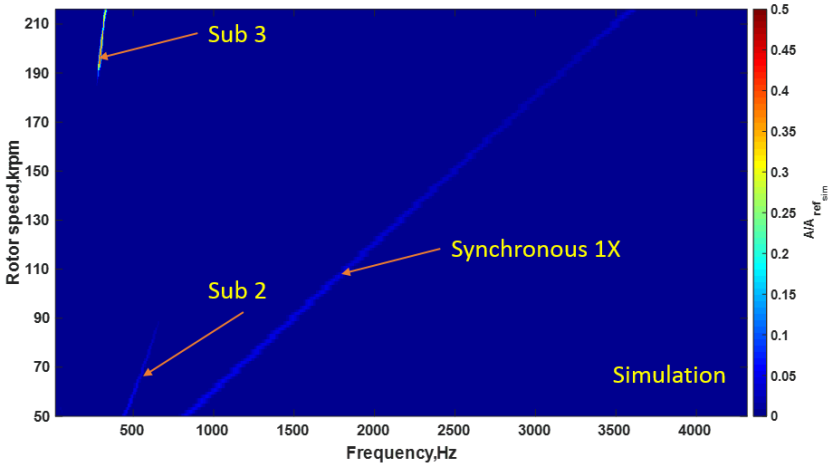

(a) Simulation results at MX

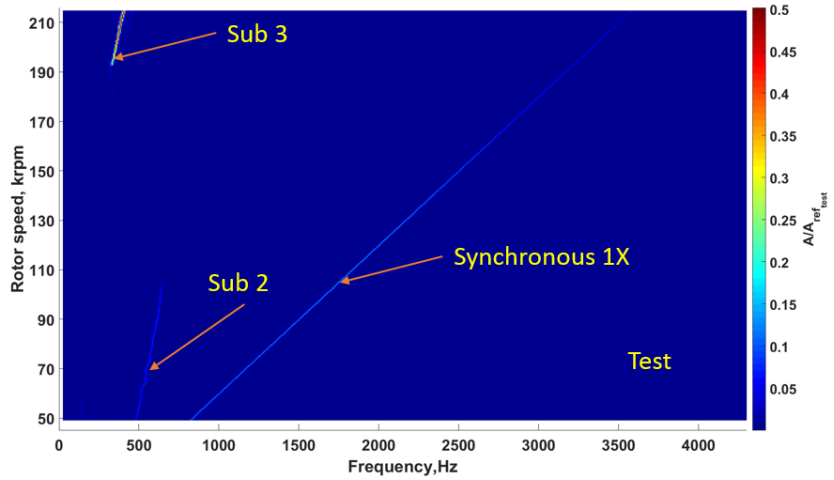

(b) Test results at MX

Figure 6 Waterfall diagrams of the simulated and measured rotor displacement at MX at the indicated shaft motion measurement point in Fig. 2 in *X*; the magnitude of the predicted and tested response are normalised by the predicted and measured maximum displacement amplitude, respectively.

Fig. 6 shows the simulated and measured results at MX (min inner clearance/max outer clearance) corner of the tolerance box. Again, it is observed that the simulated results (**Fig. 6a**) are in good agreement with the test results (**Fig. 6b**). The main characteristics of the measurement results are well captured by the simulation. Within the sub-synchronous region, differing from **Fig. 5**, the intensity of Sub 2

component becomes much lower, and it disappears below 90 krpm in simulation, although that speed is slightly higher than 90 krpm in measurement. In the mid speed range, the rotor displacement is only dominated by synchronous component given by rotor unbalance, which means the rotor-FRB system is stable. At approximately 190 krpm, Sub 3 takes place and dominates the rotor response until reaching the top speed.

From this example, it is clearly seen that the variation of bearing inner/outer clearance leads to drastically different dynamic behaviour of TC rotor-FRB system. The nonlinear transient simulation even using the analytically calculated bearing force model gave promising correlation to the shaft motion measurements. Following the proposed method for stability optimisation, the derived bearing design showed acceptable level of rotor response across the entire speed range.

5. Conclusions

In order to develop a time-saving and accurate procedure for TC rotor-FRB system development, this paper demonstrates that the traditional linear stability analysis method can be used as a valuable pilot analysis tool to perform qualitative bearing stability optimisation. The linearly predicted results are validated through nonlinear transient simulations at selected design points across the defined parameter space. Within the indicated optimal region, a bearing design considering dimensional tolerance can be derived, and nonlinear transient simulation can then be used to obtain desired quantitative information, such as the exact level of shaft displacement. Finally, the chosen design is verified by a good correlation between simulation and shaft motion measurement. This unified combination of linear stability analysis and nonlinear transient simulation method can significantly reduce the needed time and number of test iterations during TC rotor-FRB system development, and can lead to improved TC rotor-FRB designs.

Acknowledgement

Special thanks are given to Nicholas Hylton in Cummins Turbo Technologies, UK for his effort to collect all the measurement data.

Reference List

1. Nguyen-Schäfer H. Rotordynamics of automotive turbochargers. Springer; 2015.
2. San Andrés L, Rivadeneira JC, Chinta M, Gjika K, LaRue G. Nonlinear rotordynamics of automotive turbochargers: predictions and comparisons to test data. J Eng Gas Turbines Power. 2007;129(2):488–493.
3. San Andres L, Rivadeneira JC, Gjika K, Groves C, LaRue G. Rotordynamics of small turbochargers supported on floating ring bearings—highlights in bearing analysis and experimental validation. J Tribol. 2007;129(2):391–397.
4. Schweizer B, Sievert M. Nonlinear oscillations of automotive turbocharger turbines. J Sound Vib. 2009;321(3):955–975.
5. Schweizer B. Dynamics and stability of turbocharger rotors. Arch Appl Mech. 2010;80(9):1017–1043.
6. Tian L, Wang WJ, Peng ZJ. Dynamic behaviours of a full floating ring bearing supported turbocharger rotor with engine excitation. J Sound Vib. 2011;330(20):4851–4874.
7. Tian L, Wang WJ, Peng ZJ. Effects of bearing outer clearance on the dynamic behaviours of the full floating ring bearing supported turbocharger rotor. Mech Syst Signal Process. 2012;31:155–175.
8. Tian L, Wakelin M, Lancaster C, Lindsay M. The effect of oil film instability on power losses prediction of a turbocharger rotor-fully floating ring bearing system.

In: 12th International Conference on Turbochargers and Turbocharging. London; 2016.
9. Schweizer B. Oil whirl, oil whip and whirl/whip synchronization occurring in rotor systems with full-floating ring bearings. Nonlinear Dyn. 2009;57(4):509–532.
10. Chasalevris A. Finite length floating ring bearings: Operational characteristics using analytical methods. Tribol Int. 2016;94:571–590.
11. Schweizer B. Total instability of turbocharger rotors—physical explanation of the dynamic failure of rotors with full-floating ring bearings. J Sound Vib. 2009;328(1):156–190.
12. Boyaci A, Seemann W, Proppe C. Bifurcation analysis of a turbocharger rotor supported by floating ring bearings. In: IUTAM Symposium on Emerging Trends in Rotor Dynamics. Springer; 2011. p. 335–347.
13. Tian L, Wang WJ, Peng ZJ. Nonlinear effects of unbalance in the rotor-floating ring bearing system of turbochargers. Mech Syst Signal Process. 2013;34(1):298–320.
14. Friswell MI. Dynamics of rotating machines. Cambridge University Press; 2010.
15. Chen WJ. Practical Rotordynamics and Fluid Film Bearing Design. Trafford On Demand Pub; 2015.
16. Inagaki M, Kawamoto A, Abekura T, Suzuki A, Rübel J, Starke J. Coupling analysis of dynamics and oil film lubrication on rotor-floating bush bearing system. J Syst Des Dyn. 2011;5(3):461–473.